



Pharmaceutical Nanotechnology

Synthesis, characterization of chitosan–tripolyphosphate conjugated chloroquine nanoparticle and its in vivo anti-malarial efficacy against rodent parasite: A dose and duration dependent approach

Satyajit Tripathy^a, Sabyasachi Das^a, Subhankari Prasad Chakraborty^a, Sumanta Kumar Sahu^b, Panchanan Pramanik^b, Somenath Roy^{a,*}

^a Immunology and Microbiology Laboratory, Department of Human Physiology with Community Health, Vidyasagar University, Midnapore 721102, West Bengal, India

^b Nanomaterials Laboratory, Department of Chemistry, Indian Institute of Technology, Kharagpur 721302, West Bengal, India

ARTICLE INFO

Article history:

Received 26 March 2012

Received in revised form 17 May 2012

Accepted 21 May 2012

Available online 1 June 2012

Keywords:

Malaria
Chitosan
Tripolyphosphate
Nanochloroquine
Anti-malarial drug
Plasmodium berghei

ABSTRACT

Various strategies to deliver antimalarials using nanocarriers have been evaluated. However, taking into account the peculiarities of malaria parasites, the focus is placed mainly polymer-based chitosan nanocarriers. Our purpose of the study is to develop chitosan–tripolyphosphate (CS–TPP) nanoparticles (NPs) conjugated chloroquine in application for attenuation of *Plasmodium berghei* infection in Swiss mice. NPs were prepared by ionotropic gelation between CS and sodium TPP. In the study, the interaction of CS and TPP and the presence of chloroquine at the surface of chitosan–TPP NPs have been investigated by means of different methods like FTIR, DLS, and zeta potential. After drug preparation, effective dose of the nanoconjugated chloroquine (Nch) among 100, 250, and 500 mg/kg bw/day, was studied against *P. berghei* infection in Swiss mice by blood smear staining and biochemical assay of different inflammatory markers, and antioxidant enzyme levels also performed. After evaluating the effective dose, dose-dependent duration study was performed for 5, 10, 15 days. From the present study the maximum effect of Nch was found at 250 mg/kg bw concentration for 15 days treatment. So, this Nch might have potential of application as therapeutic anti-malarial and antioxidant agent.

© 2012 Elsevier B.V. All rights reserved.

1. Introduction

Pharmaceuticals and pharmaceutical carriers represent currently an important and still growing area of biomedical research by the help of the basic property of any multifunctional nanocarrier. Nanotechnology is a multidisciplinary field covering the design, manipulation, characterization, production and application of structures, devices and systems at nanometer scale (1–500 nm size range) which at this size range present with unique or superior physicochemical properties (Bawa et al., 2005). Chitin is an interesting biopolymer to prepare nano sized particle, owing to

Abbreviations: CRP, C-reactive proteinase; DTNB, 5',5'-dithio(bis)-2-nitrobenzoic acid; EDTA, ethylene diamine tetra acetate; GR, glutathione reductase; GSH, reduced glutathione; GSSG, oxidized glutathione; H₂O₂, hydrogen peroxide; IC, infected control; LDH, lactate dehydrogenase; MDA, malondialdehyde; MPO, myeloperoxidase; NADPH, nicotinamide adenine dinucleotide phosphate; Nch, nanochloroquine; OPD, O-diaminidine; PBS, phosphate buffer saline; ROS, reactive oxygen species; SGOT, serum glutamate oxalate transaminase; SGPT, serum glutamate pyruvate transaminase; TBA, thiobutiric acid; TBARS, thiobutiric acid reactive substance; TCA, trichloro acetic acid; TrxR, thioredoxine reductase.

* Corresponding author. Tel.: +91 3222 275329; fax: +91 3222 275329.

E-mail address: sroy.vu@hotmail.com (S. Roy).

its unique polymeric cationic character, good biocompatibility, biodegradability, its mucoadhesivity, and absorption-enhancing effects. Additionally, the use of a natural polymer as the carrier material avoids any potentially toxic effects of nanoparticles (Wang et al., 2012). Chitosan, a natural linear biopolyaminosaccharide obtained by alkaline deacetylation of chitin (Fig. 1a), and second abundant polysaccharide next to cellulose. Rendering amino (–NH₂) and hydroxyl (–OH) groups, CS enables a high degree of chemical modification. Chitin is a straight chain homopolymer composed of (1,4)-linked N-acetyl glucosamine units, while CS comprises of copolymers of glucosamine and N-acetyl glucosamine. CS has one primary amino group and two free hydroxyl groups for each C6 building unit. Due to the availability of free amino groups, it carries a positive charge and reacts with many negatively charged surfaces such as the cell membrane, mucus lining (due to negatively charged sialic acid residues), and also with other anionic polymers (Paliwal et al., 2012; Chakraborty et al., 2010). CS is a weak base, insoluble in water and organic solvents, however, it is soluble in dilute aqueous acidic solution (pH < 6.5), which can convert the glucosamine units into a soluble form of protonated amine (R–NH₃⁺) (Lam et al., 2006). As such nanomedicine drug delivery system can reduce the drug dosage frequency, treatment time and toxicity (Swai et al., 2008). Thus nanodrug delivery systems

seem to be a promising and viable strategy for improving malaria treatment.

Both passive and active nanotechnology-based drug delivery systems for malaria have been evaluated and they are able to deliver the drug to the specific target in the human body where the malaria parasite is located. In passive targeting, conventional nanocarriers or surface-modified long-circulating nanocarriers can be used (Kato et al., 2003; Soma et al., 2000). Although it is true that the pharmacokinetics of drugs differ between humans and mice, it is also true that all mammalian plasmodium species have comparable life cycles and are sensitive to the same drugs. The increasing resistance of malaria parasites to available drugs increases the burden of disease and the need to develop new and effective anti-malarial agents (Guinovart et al., 2006). The outbred albino mouse inoculated with *Plasmodium berghei* is generally considered to be a valid model for the primary and large scale screening of drugs for eventual use against human malaria. The use of strains of rodent malaria parasites can yield additional information concerning both its potential value against strains of human malaria, and the mode of action of a compound. Therefore, a credible *in vivo* screening system needs to be established for testing the efficacy of these drugs against malaria (Peters et al., 1975).

The antimalarial drug policy states that all *Plasmodium vivax* cases, undiagnosed fever cases, and clinical malaria cases should be treated with chloroquine in full therapeutic doses. Chloroquine, an effective drug on all five species of parasites, including some strains of *Plasmodium falciparum*, therefore, remains the main drug for the treatment of all malarias in India except in PHCs with 10% or more cases found resistant to it (Sharma, 2007). CQ acts against the intraerythrocytic stage of the human malaria parasite, and is thought to exert its toxic effect in the parasite's acidic digestive vacuole (DV). Once inside the acidic DV, CQ becomes protonated (mostly diprotonated), which renders it less membrane-permeant and results in its accumulation to high concentrations but CQ become ineffective due to efflux out of the DV, away from its primary site of accumulation and action (Lehane and Kirk, 2010). In this fact, nano drug carrier may overcome the efflux of CQ from DV and as well as may reduce the resistant zone of the age old CQ.

This study seeks to synthesize, characterize the CS-TPP nanoparticle conjugated chloroquine and to determine whether the initial number of parasites inoculated and/or the medication after inoculation influence the anti-malarial efficacy of nanoconjugated chloroquine against *P. berghei* NK65 infection in Swiss mice as models, in order to ascertain the true value of its use in the treatment of malaria.

2. Materials and methods

2.1. Parasites

The NK65 strain of *P. berghei*, used in this study was supplied from Dr. Pralhad Ghosh's Research Laboratory, Department of Biotechnology, Delhi University, South Campus, Delhi, India and maintained into sex and age-matched wild type mice by weekly passage by intraperitoneal injection (Joshi et al., 2008) and blood stage parasites were stored at -80°C .

2.2. Animals

Swiss male mice (6–8 weeks old, weight 20–25 g) were used to full fill the experiments. Animals were maintained in accordance with the guidelines of the National Institute of Nutrition, Indian Council of Medical Research, Hyderabad, India, and approved by the ethical committee of Vidyasagar University. The animals were fed standard pellet diet with vitamins, antibiotic and water were

given *ad libitum* and housed in polypropylene cage (Tarson) in the departmental animal house with 12 h light and dark cycle under standard temperature ($25 \pm 2^{\circ}\text{C}$). The animals used in this study did not show any sign of malignancy or other pathological processes.

2.3. Chemicals and reagents

Tris buffer, sodium chloride (NaCl), Triton-X 100, potassium dihydrogen phosphate (KH_2PO_4), dipotassium hydrogen phosphate (K_2HPO_4), ethylene diamine tetra acetate (EDTA), sodium hydroxide (NaOH), chloroform, sodium acetate, ammonium acetate, potassium hydroxide (KOH), methanol, Gimsa, Tris-HCl, formaldehyde, alcohol, diphenylamine (DPA) were procured from Merck Ltd., SRL Pvt. Ltd., Mumbai, India. 5',5'-dithio(bis)-2-nitrobenzoic acid (DTNB), standard reduced glutathione (GSH), glutathione reductase (GR), NADPH, Na₄ NADPH, oxidized glutathione (GSSG) were procured from Sigma (St. Louis, MO, USA). Commercially available histopaque 1077, hepes, Phorbol mirested aceted (PMA), horse heart cytochrome-c, fetal calf serum, Minimal Essential Medium (MEM), Dulbecco Modified Eagle's medium (DMEM) were purchased from Sigma Chemical Co., USA. All other chemicals were from Merck Ltd., SRL Pvt. Ltd. Mumbai and were of the highest purity grade available.

2.4. Drug preparation

2.4.1. Preparation of chitosan-TPP nanoparticle

Chitosan nanoparticles were prepared by ionotropic gelation between chitosan and sodium tripolyphosphate (Shu and Zhu, 2002). The synthetic procedure involves the dissolution of 0.1 g chitosan in 100 ml of 1% acetic acid. Then three different concentrations of TPP (0.6, 1.2, 1.8 mg/ml) were prepared by dissolving respective amount of TPP in deionized water. Under magnetic stirring at room temperature, 5 ml of different concentrated TPP solution was added into 15 ml of 1 mg/ml chitosan solution drop wise to maintain chitosan to TPP weight ratio of 5:3, 5:2, 5:1 respectively. Then the reaction was stirred for 6 h. Finally the particles of different sizes were obtained depending upon chitosan to TPP weight ratio, which was collected by centrifugation at 12,000 rpm for 10 min. These particles were further purified by washing several times with deionized water followed by centrifugation. Finally these particles were dried at 60°C .

2.4.2. Particle characterization

2.4.2.1. Fourier transform infrared spectroscopy (FTIR) study. FTIR scanning was performed in transmission mode using Perkin-Elmer spectrometer equipped with a DTGS KBr detector and a KBr beam splitter with constant nitrogen purging. IR grade KBr was used as scanning matrix. One to two milligram of fine sample powder and 90–100 mg of KBr powder were mixed and dried completely, then transferred to 13 mm die to make a nearly transparent and homogeneous pallet. All spectra were taken at 4 cm^{-1} resolution, averaged over 20 scans in the range $400\text{--}4000\text{ cm}^{-1}$.

2.4.2.2. Dynamic light scattering (DLS) study of particle. Particle size was measured and analyzed with a dynamic light scattering analyzer (Malvern Instrument). The analysis was performed at scattering angle 90°C under 25°C . In brief, particle were suspended in deionized water at a concentration of 1 mg/ml then the sample was sonicate using a sonicator bath until sample was form a homogenous suspension. For size measurement by DLS, sonicated stock solution of particle (0.5 mg/ml) was diluted four times.

2.4.2.3. Zeta potential measurements of particle. The zeta (ξ) potential is the electrostatic potential that exists at the shear plane of

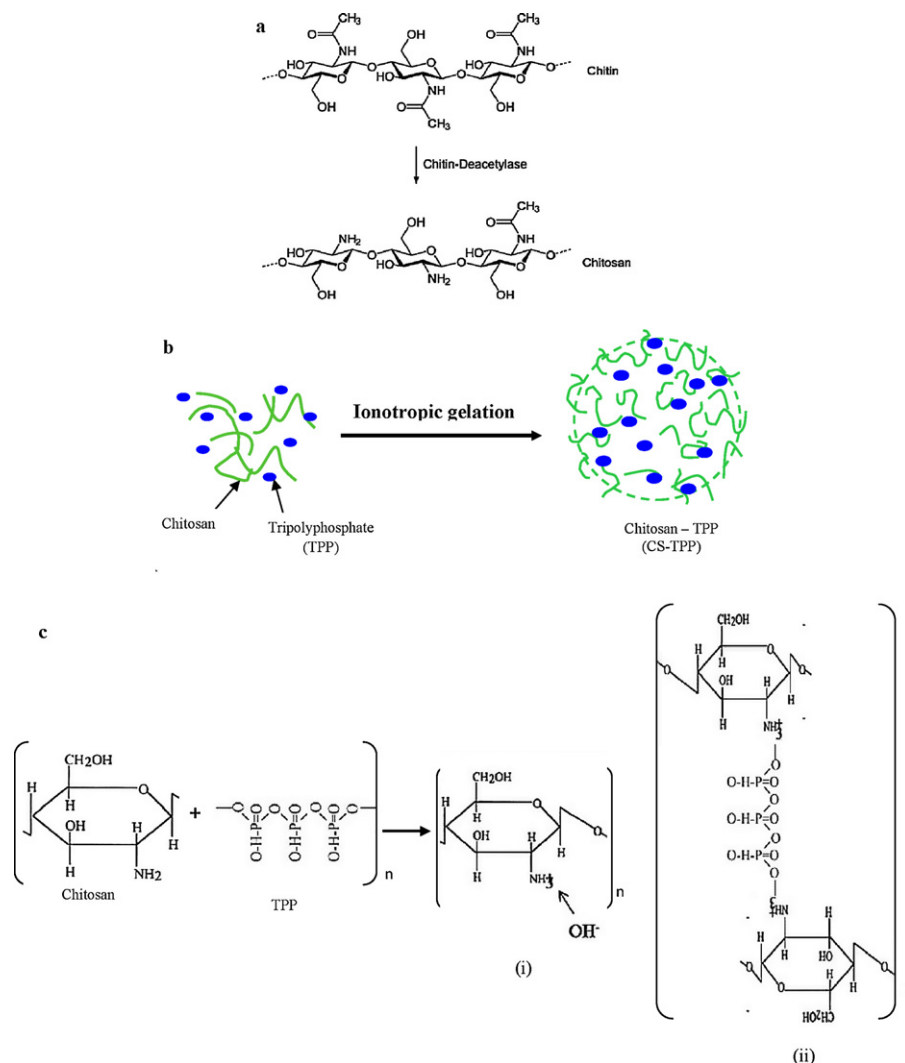


Fig. 1. Schematic representation of (a) chemical structure of chitosan, the polymer is obtained by the partial deacetylation of naturally occurring polymer, chitin; (b) the preparation of CS-TPP nanoparticle; (c) interaction mechanism of between chitosan and tripolyphosphate: (i) deprotonation; (ii) cross linking.

a particle, which is related to both surface charge and the local environment of the particle. The zeta potential of our samples was determined with a Zeta Potential Analyzer from Brookhaven Instruments Corporation. For measurement the zeta (ξ) potential value, chitosan-TPP NPs were suspended in deionized water to the concentration 0.05 mg/ml.

2.4.2.4. In vitro cyto-toxicity of chitosan-TPP nanoparticles by MTT assay. The HeLa cell lines were cultivated for in vitro experiments. Cell lines were obtained from the National Centre for Cell Sciences (NCCS) Pune, India. It was cultured in Dulbecco Modified Eagle's medium (DMEM) and Minimal Essential Medium (MEM) supplemented with 10% fetal calf serum, 100 units/ml penicillin and 100 μ g/ml streptomycin, 4 mM L-glutamine under 5% CO₂ and 95% humidified atmosphere at 37 °C. HeLa cell lines were seeded into 96 wells of tissue culture plates having 180 μ l of complete media and were incubated for 18 h. Chitosan-TPP nanoparticle was added to the cells at different concentrations were incubated for 72 h at 37 °C in a humidified incubator maintained with 5% CO₂. The cell viability was estimated by 3-(4,5-dimethylthiazol)-2-diphenyltertrazolium bromide (MTT) (Chakraborty et al., 2011a,b).

2.4.3. Loading of drug on nanoparticles and its characterization

2 mg/ml chloroquine solution was prepared by dissolving 40 mg of drug in 20 ml of deionized water. Then 3–4 drops of diluted phosphoric acid was added to above chloroquine solution. Finally, drug loaded chitosan-TPP NPs was obtained by adding 5 ml of chitosan-TPP NPs solution (1 mg/ml) in 5 ml of above drug solution. This reaction was stirred for 24 h at room temperature. Drug conjugated chitosan NPs was obtained followed by above centrifugation process and free chloroquine was discarded. Then the chloroquine encapsulated nanoparticles was dry in oven at 40 °C. Then this nanoconjugated chloroquine was taken various weights and biological study was carried out. The drug loaded NPs was characterized by FTIR, DLS and zeta potential according to the process of nanoparticle characterization.

2.4.3.1. Actual drug content and encapsulation efficiency. Actual drug content and encapsulation efficiency were measured by the method of Cevher et al. (2006). After 36 h of stirring, the mixtures were centrifuge at 3500 \times g for 10 min to get nanoconjugated chloroquine as pallet. Drug content was determined by analyzing the CS-TPP solution and pallet (dissolve in 1.0 ml PBS, pH 7.4) using Hitachi U2001 UV/Vis spectrophotometer at a wavelength

of 343 nm with PBS as reference (Takla and Dakas, 2002). Drug content was determined by comparing with the standard curve of chloroquine which was achieved from chloroquine solution in PBS (pH 7.4) with concentration between 0.001 and 0.1 mg/ml. Actual drug content (AC) and encapsulation efficiency (EE) were calculated (Eqs. (1) and (2)). All analyses were carried out in triplicate. Results are expressed as the mean percentage (w/w) \pm S.D. of three formulations. Where M_{act} is the actual chloroquine content in weighed quantity of CS-TPP, M_{ms} is the weighed quantity of powder of CS-TPP and M_{the} is the theoretical amount of chloroquine in CS-TPP calculated from the quantity added in the process.

$$AC (\%) = \frac{M_{act}}{M_{ms}} \times 100 \quad (1)$$

$$EE (\%) = \frac{M_{act}}{M_{the}} \times 100 \quad (2)$$

2.5. Parasite density determination and inoculums preparation

Standard inoculum was prepared from a donor mouse with *P. berghei* parasitized erythrocytes. Thin blood films were made by collecting blood from tail vein, this was stained with Gimsa stain and the percentage of parasitemia was determined by counting the number of parasitized red blood cells out of 1000 blood cells in 10 random microscopic fields. The parasitemia has been presented in percentage by with this formula: % of parasites = (no. of parasites in RBC/no. of RBCs) \times 100. Our interested infected blood from the donor mouse was obtained by cardiac puncture after anesthesia with chloroform. Each mouse was infected intraperitoneal with standard inoculums of the 10^6 parasitized erythrocyte suspension in phosphate buffered saline (0.2 ml) from a donor mouse that was prepared based on percentage parasitemia (Tripathy et al., 2012).

2.5.1. Effect of CS-TPP on parasitic infection

To evaluate whether CS-TPP NP itself have antimalarial activity, 100 mg/kg bw/day, 250 mg/kg bw/day and 500 mg/kg bw/day CS-TPP were treated by intraperitoneal injection to *P. berghei* infected mice for successive 10 days as per our previous published lab report (Tripathy et al., 2012). Mice were divided into 5 groups of six (6) animals each. Group I: Control; Group II: *P. berghei* infection control; Group III: *P. berghei* infection control +100 mg/kg bw/day CS-TPP; Group IV: *P. berghei* infection control +250 mg/kg bw/day CS-TPP; Group V: *P. berghei* infection control +500 mg/kg bw/day CS-TPP.

2.6. Experimental design

2.6.1. Effective dose determination study of nanoconjugated chloroquine against *P. berghei* infection

To determine the effective dose, 100 mg/kg bw/day, 250 mg/kg bw/day and 500 mg/kg bw/day nanoconjugated chloroquine were treated by intraperitoneal injection to *P. berghei* infected mice for successive 10 days (Tripathy et al., 2012). Mice were divided into 5 groups of six (6) animals each. Group I: Control; Group II: *P. berghei* infection; Group III: *P. berghei* infection +100 mg/kg bw/day nanoconjugated chloroquine (Nch); Group IV: *P. berghei* infection +250 mg/kg bw/day Nch; Group V: *P. berghei* infection +500 mg/kg bw/day Nch.

2.6.2. Effective duration determination study of nanoconjugated chloroquine against *P. berghei* infection

To determine the effective duration, *P. berghei* infected mice were injected intraperitoneal with their effective dose of Nch, respectively for 5 days, 10 days and 15 days. After sacrifice blood sample ($n=6$ /group) was used for quantification of parasitemia,

preparation of serum and separation of lymphocyte, RBC for biochemical estimation of different parameters.

2.7. Separation of serum, lymphocyte and RBC

Serum was separated by centrifugation of blood samples at $1500 \times g$ for 15 min taken without anticoagulant. Serum was kept at -80°C for the biochemical estimation of different parameters. Lymphocytes were isolated from blood heparinized blood samples using standard isolation techniques (Tripathy et al., 2012). Blood samples were diluted with equal amount of PBS (pH 7.0) buffer and then layered very carefully on the density gradient (Histopaque 1077) in 1:2 ratios. Centrifuged at $500 \times g$ for 20 min and the white milky layer of mononuclear cells, i.e., lymphocytes were carefully removed. The layer was washed twice with the same buffer and centrifuged at $3000 \times g$ for 10 min to get the required pellet of lymphocytes and rest pellet as RBC was transferred in another centrifuge tube and stored at -80°C for further study. The pellets of lymphocytes were lysed in a hypotonic lyses buffer for 45 min at 37°C and kept at -20°C until biochemical parameter experiment (Sandhu and Kaur, 2002).

2.8. Biochemical estimation

2.8.1. Superoxide anion generation

The superoxide production was measured by the SOD-inhibitable reduction of acetylated cytochrome c (Babior et al., 2002). All groups of lymphocytes were resuspended in phosphate buffer saline (PBS) supplemented with 1 mM L-NMMA (NG-methyl-L-arginine, to avoid sequestering of O_2 by nitric oxide) at 2×10^6 cells/ml. 0.1 $\mu\text{g/ml}$ phorbol 12-myristate 13-acetate (PMA), a potent stimulant, and 20 IM horse cytochrome c were added to lymphocyte suspensions. Cytochrome c reduction by generated superoxide was then monitored spectrophotometrically at 550 nm wavelength with or without the addition of 3 IM SOD. The superoxide generation assay was performed in room air conditions (Goldstein et al., 1977).

2.8.2. NADPH oxidase activity

After the isolation from control and infected blood, the lymphocytes of different groups prewarmed in Krebs ringer buffer (KRB) with 10 mM glucose at 37°C for 3 min and PMA (0.1 $\mu\text{g/ml}$) prewarmed at 37°C for 5 min was added than the reaction was stopped by putting in ice. Centrifugation was carried out at $400 \times g$ for 5 min and the resultant pellet was resuspended in 0.34 M sucrose. The cells were then lysed with hypotonic lysis buffer. Centrifugation was carried out at $800 \times g$ for 10 min and the supernatant used to determine enzyme activity. NADPH oxidase activity was determined spectrophotometrically by measuring cytochrome c reduction at 550 nm. The reaction mixture contained 10 mM phosphate buffer (pH 7.2), 100 mM NaCl, 1 mM MgCl_2 , 80 μM cytochrome c, 2 mM NaN_3 and 100 μl of supernatant (final volume 1.0 ml). A suitable amount of NADPH (10–20 μl) was added last to initiate the reaction (Heyneman and Vercauteren, 1984).

2.8.3. Nitrite generation (NO) and release

No generation and release was measured according to Chakraborty et al. (2011a,b) using Griess reagent (containing 1 part of 1% sulfanilamide in 5% phosphoric acid, and 1 part of 0.1% of N-C-1 naphthyl ethylene diamine dihydrochloride). Reading was taken in a UV spectrophotometer at 546 nm. The levels of NO were expressed as $\mu\text{mol/mg}$ protein.

2.8.4. C-reactive protein (CRP) level

C-reactive protein level in serum was estimated using a sandwich ELISA Kit (Tulip, Mumbai, India). The assay was performed as

per the detailed instructions of the manufacturer. The levels of CRP were expressed as $\mu\text{g}/\text{dl}$.

2.8.5. Lactose dehydrogenase (LDH) activity

LDH activity in serum was estimated using a sandwich ELISA Kit (Tulip, Mumbai, India). The assay was performed as per the detailed instructions of the manufacturer. The activity of LDH was expressed as $\mu\text{g}/\text{dl}$.

2.8.6. Serum glutamate oxalate transaminase (SGOT) and serum glutamate pyruvate transaminase (SGPT) activity

To measure enzymes SGOT and SGPT in serum, a modified protocol of the standard colorimetric end-point method was used (Reitman and Frankel, 1957). Briefly, $20\ \mu\text{l}$ of serum was added to $100\ \mu\text{l}$ of reaction mixture in PBS, mixed, and incubated ($37\ ^\circ\text{C}$, 60 min and 30 min respectively), followed by the addition of $100\ \mu\text{l}$ of 2,4-dinitrophenylhydrazine. The mixture was incubated for an additional 20 min at room temperature. The reaction was stopped by addition of 1 ml of 0.4 M NaOH and absorbance was read at 520 nm after 5 min.

2.8.7. Myeloperoxidase (MPO) activity in serum

$200\ \mu\text{l}$ of serum was reacted with $200\ \mu\text{l}$ substrate (containing H_2O_2 and OPD) in dark for 30 min. The blank was prepared with citrate phosphate buffer (pH 5.2) and substrate, in absence of cell free supernatant. The reaction was stopped with addition of $100\ \mu\text{l}$ 2(N) sulfuric acid and reading was taken at 492 nm in a spectrophotometer (Chakraborty et al., 2011a,b).

2.8.8. Lipid peroxidation (MDA) level

The extent of lipid peroxidation was estimated as the concentration of thiobarbituric acid reactive product malondialdehyde

(MDA) by using the method of Chakraborty et al. (2011a,b). One hundred microliters of sample was added to $100\ \mu\text{l}$ of double-distilled water and $50\ \mu\text{l}$ of 8.1% sodium dodecyl sulfate (SDS) and incubated at room temperature for 10 min. Three hundred and seventy-five microliters of 20% acetic acid (pH 3.5), along with $375\ \mu\text{l}$ of thiobarbituric acid (0.6%), was added to the tissue solution and placed in a boiling water bath for 60 min. After incubation, $250\ \mu\text{l}$ of double-distilled water and 1.25 ml of 15:1 butanol-pyridine solution were added to the mixture and centrifuged for 5 min at $2000 \times g$. The supernatant was removed and measured at 530 nm with the use of the Hitachi U-2000 spectrophotometer. Malondialdehyde concentrations were determined by using 1,1,3,3-tetraethoxypropane as standard.

2.8.9. Thioredoxin reductase activity (TrxR)

By using the method of Holmgren and Bjorsnstedt (1995) thioredoxin reductase (TrxR) activity was measured by the reduction of dithionitrobenzene (DTNB) in the presence of di-nucleotide phosphate reduced (NADPH). After initiating the reaction with NADPH, the increase in absorbance was monitored at 412 nm at room temperature and specific activity was calculated as units of enzyme per mg protein. The reaction mixture contained 100 mM potassium phosphate buffer (PBS), pH 7.5, 2 mM EDTA, 3 mM DTNB, 0.2 mM NADPH.

2.8.10. Hemolytic activity

Hemolytic activity was measured by using the method of Gupta and Saxena (1980). In briefly the aliquot samples of the parasite preparations were mixed with 0.5 ml of normal erythrocyte suspension in small tubes and the final volume was made to 2.0 ml with 0.15 M saline and was incubated at $37\ ^\circ\text{C}$ for 30 min. Then it was centrifuged at $2000 \times g$ for 10 min later the supernatant was

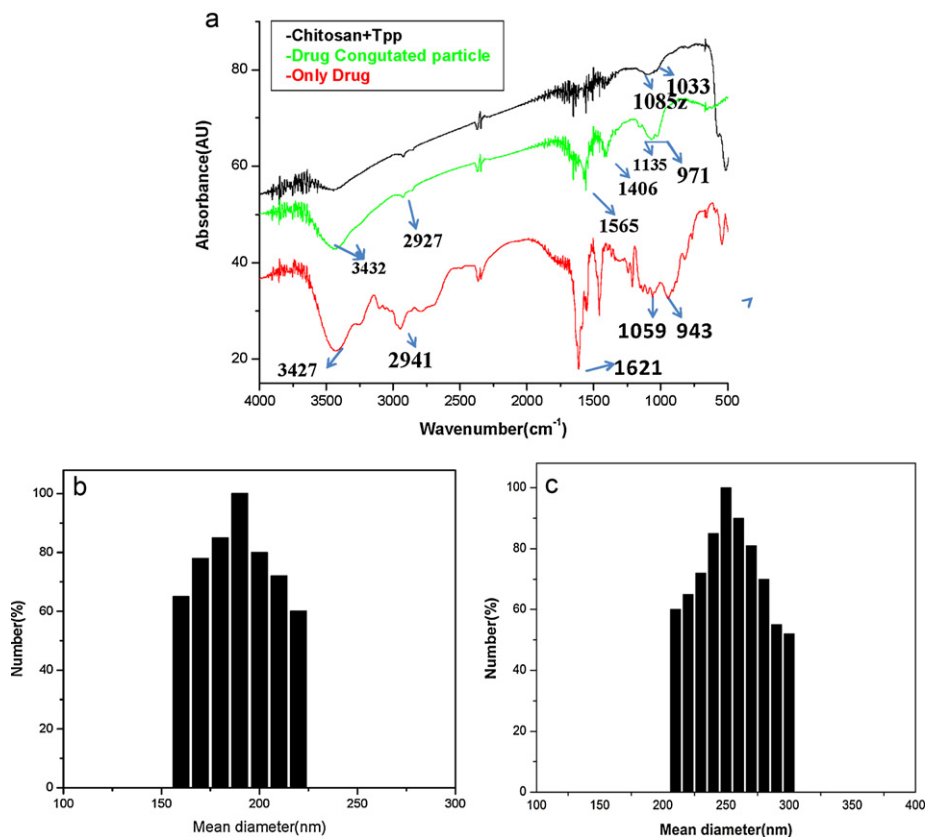


Fig. 2. The FT-IR spectra (a) of the chitosan-TPP, chloroquine loaded chitosan-TPP and the chloroquine. The dynamic light scattering study (DLS) study of the (b) chitosan-TPP nano particle; (c) chloroquine loaded chitosan-TPP nano particle.

measured at 540 nm and the parasite was substituted by saline against a reagent blank.

2.8.11. Determination of reduced glutathione (GSH)

Reduced glutathione estimation in the cell lysate was performed by the method of Chakraborty et al. (2011a,b). The required amount of the cell lysate was mixed with 25% of trichloroacetic acid and centrifuged at $2000 \times g$ for 15 min to settle the precipitated proteins. The supernatant was aspirated and diluted to 1 ml with 0.2 M sodium phosphate buffer (pH 8.0). Later, 2.0 ml of 0.6 mM DTNB was added. After 10 min it was measured at 405 nm. A standard curve was obtained with standard reduced glutathione. The level of GSH was expressed as $\mu\text{g}/\text{mg}$ protein.

2.8.12. Oxidized glutathione level (GSSG)

The oxidized glutathione level was measured after derivatization of GSH with 2-vinylpyridine according to the method of Chakraborty et al. (2011a,b). In brief, with 0.5 ml cell lysate, 2.0 μl of 2-vinylpyridine was added and incubates for 1.0 h at 37°C . Then the mixture was deproteinized with 4% sulfosalicylic acid and centrifuged at $1000 \times g$ for 10 min to settle the precipitated proteins. The supernatant was aspirated and GSSG level was estimated with the reaction of DTNB at 412 nm in spectrophotometer and calculated with standard GSSG curve. The level of GSSG was expressed as $\mu\text{g}/\text{mg}$ protein.

2.8.13. Redox ratio (GSH/GSSG)

Redox ratio was determined for all the five groups by taking the ratio of reduced glutathione/oxidized glutathione.

2.8.14. Activity of glutathione reductase (GR)

The GR activity was measured by the method of Chakraborty et al. (2011a,b). The tubes for enzyme assay were incubated at 37°C and contained 2.0 ml of 9 mM GSSG, 0.02 ml of 12 mM NADPH, Na_4 , 2.68 ml of 1/15 M phosphate buffer (pH 6.6) and 0.1 ml of cell lysate. The activity of this enzyme was determined by monitoring the decrease in absorbance at 340 nm. The activity of GR was expressed in terms of nmol NADPH consumed/min/mg protein.

2.8.15. Activity of catalase (CAT)

Catalase activity was measured in the cell lysate by the method of Chakraborty et al. (2011a,b). The final reaction volume of 3 ml contained 0.05 M Tris-buffer, 5 mM EDTA (pH 7.0), and 10 mM H_2O_2 (in 0.1 M potassium phosphate buffer, pH 7.0). About 50 μl aliquot of the lysates were added to the above mixture. The rate of change of absorbance per min at 240 nm was recorded. Catalase activity was calculated by using the molar extinction coefficient of $43.6 \text{ M}^{-1} \text{ cm}^{-1}$ for H_2O_2 . The level of catalase was expressed in terms of mmol H_2O_2 consumed/min/mg protein.

2.8.16. Activity of superoxide dismutase (SOD)

SOD activity was determined from its ability to inhibit the auto-oxidation of pyrogallol according to Chakraborty et al. (2011a,b). The reaction mixture consisted of 50 mM Tris (hydroxymethyl) aminomethane (pH 8.2), 1 mM diethylenetriamine pentaacetic acid, and 20–50 μl of cell lysate. The reaction was initiated by addition of 0.2 mM pyrogallol, and the absorbance measured kinetically at 420 nm at 25°C for 3 min. SOD activity was expressed as unit/mg protein.

2.9. Protein estimation

Protein was determined according to Lowry et al. (1951) using bovine serum albumins as standard.

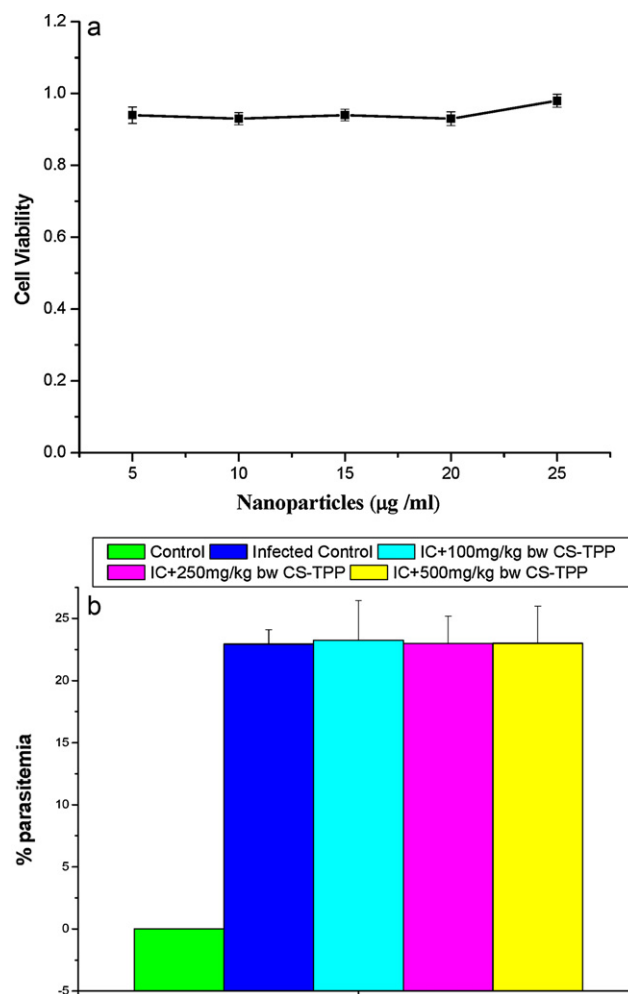


Fig. 3. Graphical presentation of (a) in vitro cyto-toxicity of chitosan-TPP nanoparticles by MTT assay and (b) in vivo antimalarial activity of CS-TPP nano particle.

2.10. Statistical analysis

The data were expressed as mean \pm SEM, $n=6$. Comparisons of the means of control, and experimental groups were made by Student's *t*-tests (using a statistical package, Origin 6.1, Northampton, MA 01060, USA), $P < 0.05$ as a limit of significance.

3. Results and discussion

Nanomedicine has the potential to restore the use of old and toxic drugs by modifying their biodistribution, improve bioavailability and reducing toxicity (Peters et al., 1975), so we have synthesized and characterized by conjugating the chloroquine with CS-TPP NPs and it has been treated 100 mg/kg bw/day, 250 mg/kg bw/day and 500 mg/kg bw/day in *P. berghei* infected Swiss mice to evaluate the effective dose. To determine the effective duration, we have charged the evaluated effective dose for 5 days, 10 days and 15 days in *P. berghei* infected Swiss mice after 10 days successive infection.

3.1. Particle characterization

For certain period, drug delivery formulation based on CS was usually prepared by chemically cross linking agents such as glutaraldehyde which was responsible to induce toxicity. However, to overcome this disadvantage low molecular weights anion,

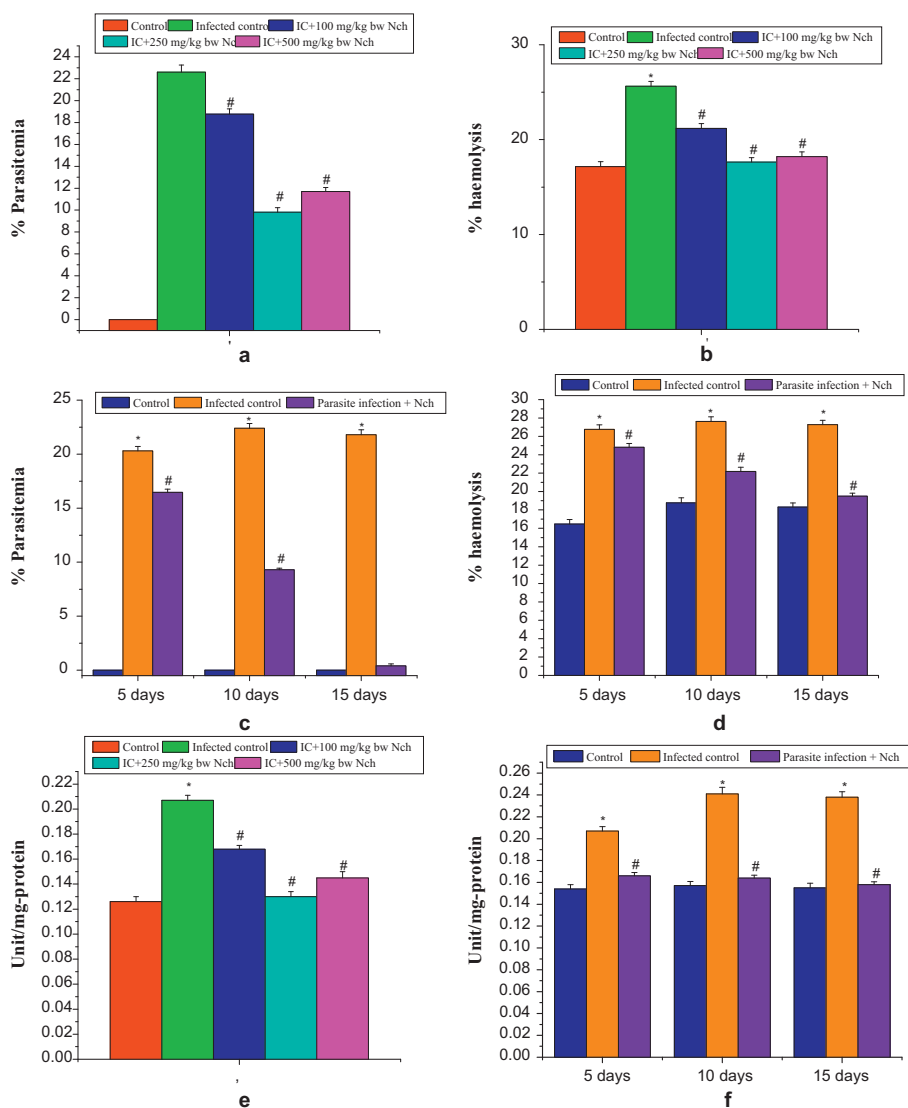


Fig. 4. Graphical presentation of parasitemia (a and c); hemolytic activity (b and d) and thioredoxin reductase activity (e and f) during effective dose and effective duration study respectively. Values are expressed as mean \pm SEM, $n=6$. *Significant difference ($P<0.05$) compared to control group. #Significant difference ($P<0.05$) compared to infected control group.

TPP were applied in the formulation preparation via electrostatic interaction (Lam et al., 2006). In the study, chloroquin was incorporated in nano-particle during the synthesis of CS-TPP. All these particles are characterized by FTIR spectroscopy, DLS, zeta potential.

Cationic CS could react with multivalent counter ions to form the intermolecular and/or intramolecular network structure by ionic interaction between NH_3^+ protonated groups and negatively charged counter ions of TPP. Due to hydrolysis, the small molecule polyelectrolyte, sodium TPP, dissociate in water and released out OH^- ions, so both OH^- and $\text{P}_3\text{O}_{10}^{5-}$ ions coexisted in the TPP solution and could ionically react with NH_3^+ of CS (Fig. 1c). The present study has been performed by FTIR spectroscopy for the comparison of FTIR spectra of the CS-TPP, CS-TPP loaded chloroquin and chloroquin (Fig. 2a). The chloroquin loaded chitosan NPs reveals one most important peak at 1565 cm^{-1} that assigned to $\text{N}=\text{O}$ stretching of amine presence in drug. The peak at 2927 cm^{-1} was attributing C-H stretching of methylene group. The skeleton bands of heterocyclic aromatic ring appears in the region 1565 cm^{-1} and 1406 cm^{-1} stretching vibrations of $\text{C}=\text{C}$, $\text{C}=\text{N}$ which indicated the presence of chloroquin on chitosan NPs.

The particle size has been established by DLS. Fig. 2b and c shows respectively the particle size of the chitosan-TPP NP and drug loaded nanoparticles. After analyzing data, it was found that chitosan-TPP nanoparticle size was in the range of 150–225 nm and the drug loaded nanoparticles size was in the range of 150–300 nm. The highest fraction of chloroquin NP present in the solution was of less than 250 nm.

Chitosan-TPP nanoparticles are mainly characterized by a positive zeta potential. Interaction is therefore strong towards any negative surface charge. We also studied the zeta potential of the CS-TPP NPs and Nch. The positive charge of Nch (+32.9 mV) was slightly higher than CS-TPP NPs (+30 mV). This is due to presence of positively charge amine group present in drug molecule.

The cytotoxic activity of chitosan-TPP nanoparticle on HeLa cell lines was evaluated by assessing the cell viability using a standard MTT assay method. Different concentration of chitosan-TPP NPs (5–25 $\mu\text{g/ml}$) was added to cells for 24 h. It was found that there was no significant difference in cell viability between the cells treated with chitosan-TPP NPs (Fig. 3a). Hence this chitosan-TPP NPs is expected to be safe for biomedical applications.

Table 1Actual drug content and encapsulation efficiency of chloroquine loaded CS–TPP nanoparticle. Values are expressed as percentile \pm S.D., $n = 6$.

Polymer	Drug	Polymer:drug ratio	Actual drug content % \pm S.D.	Theoretical drug content (%)	Encapsulation efficiency % \pm S.D.
CS–TPP	Chloroquine	1:1	27.36 \pm 1.014	50.00	54.72 \pm 1.342

Nanoconjugated chloroquine was successfully prepared in polymer:drug ratio of 1:1. Actual drug content was approximately 28% and the encapsulation efficiency was over 54% (Table 1).

It has also been found that CS–TPP NP itself have no antimalarial activity against *P. berghei*. As 100 mg/kg bw, 250 mg/kg bw and 500 mg/kg bw CS–TPP NP was administered in 10 days successive infected mice but parasitemia reduction was not observed (Fig. 3b).

3.2. Effective dose and duration determination of nanoconjugated chloroquine against *P. berghei* infection

Plasmodium infection leads to increased oxidative stress in the vertebrate hosts. The high proliferation rate of parasites

results in the production of large quantities of toxic redox-active by-products (Romao et al., 2006). Reactive oxygen species (ROS) are generated within the infected RBC (iRBC) as a result of degradation of hemoglobin in the food vacuole of the parasite (Becker et al., 2004). So, parasitemia and hemolytic activity was observed in both to evaluate the effective dose and to determine the dose dependent effective duration study. These were decreased significantly ($P < 0.05$) by 16.99%, 56.63%, 48.23% and 23.48%, 31.18%, and 28.92% respectively after 100 mg/kg bw/day, 250 mg/kg bw/day, 500 mg/kg bw/day Nch treatment respectively (Fig. 4a and b). After duration study the reduction of parasitemia was 18.91%, 58.48%, 98.16% and hemolytic activity decreased significantly ($P < 0.05$) by 7.28%, 19.65%, 28.55% (Fig. 4c and d). However, the result of Nch

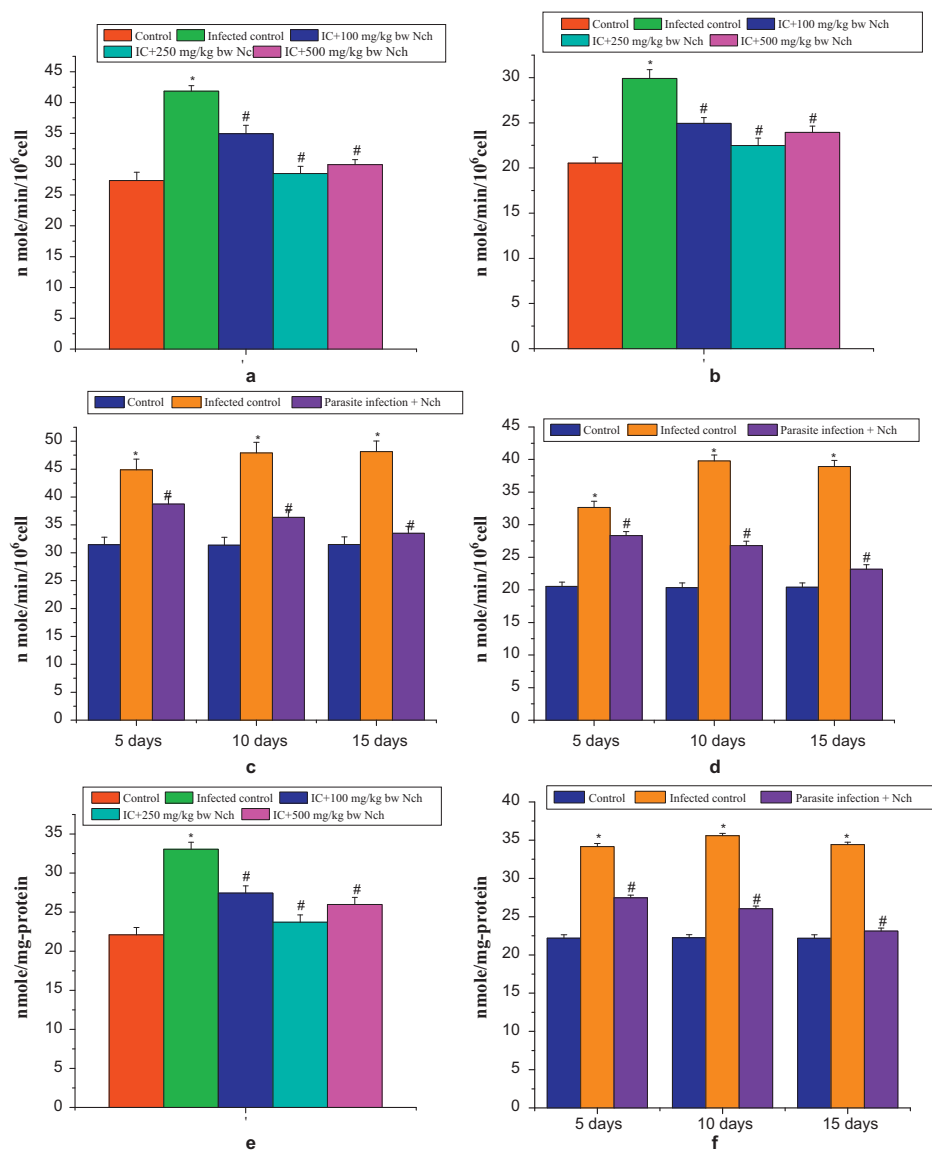


Fig. 5. Graphical presentation of superoxide radical generation (a and c); NADPH oxidase activity (b and d); lipid peroxidation (MDA level) (e and f) of lymphocytes during effective dose and effective duration study respectively. Values are expressed as mean \pm SEM, $n = 6$. *Significant difference ($P < 0.05$) compared to control group. #Significant difference ($P < 0.05$) compared to infected control group.

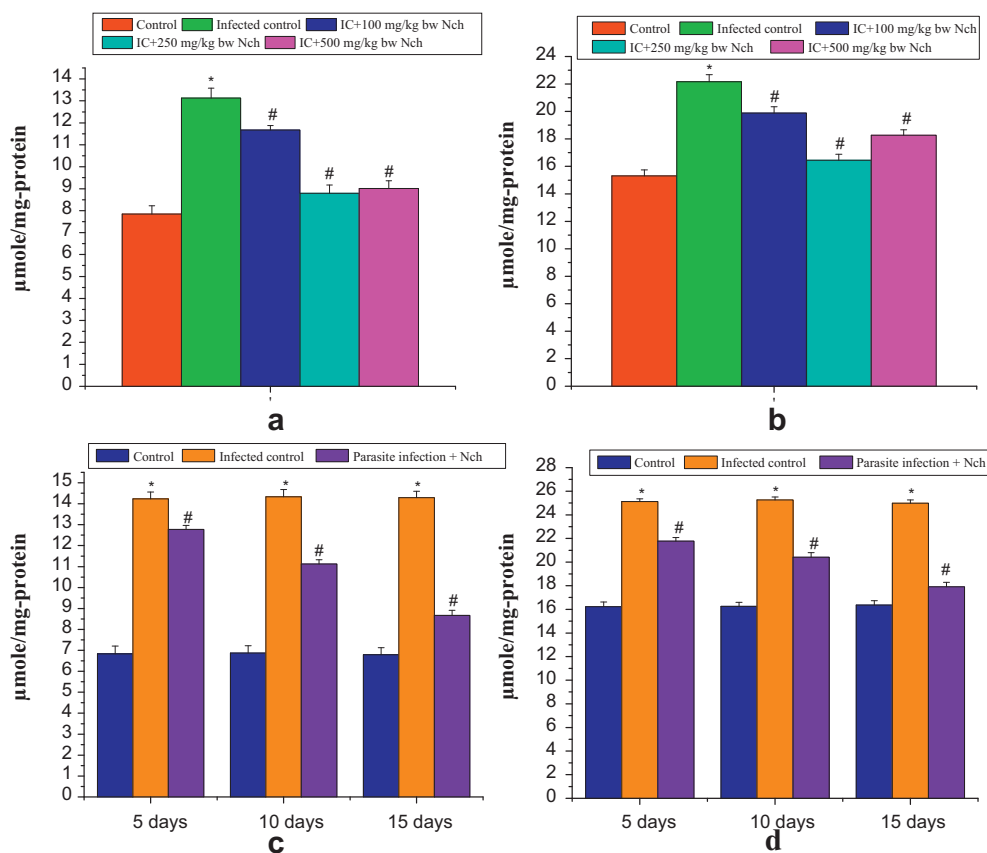


Fig. 6. Graphical presentation of nitric oxide generation of lymphocyte and nitric oxide release serum (a and b) and (c and d) during effective dose and effective duration study respectively. Values are expressed as mean \pm SEM, $n=6$. *Significant difference ($P<0.05$) compared to control group. #Significant difference ($P<0.05$) compared to infected control group.

treatment suggests that a complex relationship exists between the parasite load and the efficacy of the drug. Hemoglobin proteolysis in intraerythrocytic malaria parasites is a biochemical event. The oxidant haeme group is separated from globin chains, a process in which Fe^{2+} is oxidized to Fe^{3+} and electrons produced react with molecular oxygen to form oxygen radicals (Mohan et al., 1992; Francis et al., 1997). Our data suggested that hemolytic activity and parasitemia markedly decreased at 250 mg/kg bw/day Nch for 15 days treatment.

During infection, TrxR is responsible for transferring of electrons from NADPH to thioredoxin to contribute the antioxidant capacity of the cell. Plasmodium TrxR differs significantly from mammalian counterpart. Thioredoxin functions as redox messenger in parasite maintaining reduced intracellular environment (Mohan et al., 1992). Our result also reveals that TrxR activity also significantly ($P<0.05$) increased by 64.28% in infected groups as compared with control, in Nch treated groups it decreased significantly ($P<0.05$) as compared to infected group and maximally the activity decreased by 37.19% at 250 mg/kg bw/day Nch treatment (Fig. 4e). In case of duration study, TrxR activity increased 34.41%, 53.5%, 53.54% in infected control group respectively, but nanoconjugated chloroquine decreased TrxR activity significantly ($P<0.05$) by 19.8%, 31.95%, 33.61%; after 5 days, 10 days and 15 days treatment, respectively (Fig. 4f).

Superoxide anion ($\text{O}_2^{\bullet-}$) generation and NADPH oxidase activity in lymphocytes was significantly ($P<0.05$) increased in *P. berghei* infected group by 53.05% and 45.73% respectively. But nanoconjugated chloroquine (Nch) treatment decreased the $\text{O}_2^{\bullet-}$ generation and NADPH oxidase activity, as compared to infected control.

100 mg/kg bw Nch supplementation decreased the $\text{O}_2^{\bullet-}$ generation 9.31%, NADPH oxidase activity 16.65% and 500 mg/kg bw Nch supplementation decreased the $\text{O}_2^{\bullet-}$ generation 28.43% and NADPH oxidase activity 19.96%, and 250 mg/kg bw Nch reduced the $\text{O}_2^{\bullet-}$ generation 31.88% and NADPH oxidase activity 24.80% maximally as compared to their infected groups (Fig. 5a and b). During duration study we also found, superoxide generation and NADPH oxidase activity were increased significantly ($P<0.05$) by 42.62%, 52.75%, 52.92% and 59.11%, 95.57%, 90.73% in *P. berghei* infected group, respectively, after 5 days, 10 days and 15 days of infection. Treatment of 250 mg/kg bw/day nanoconjugated chloroquine in infected group decreased $\text{O}_2^{\bullet-}$ generation and NADPH oxidase activity significantly ($P<0.05$) by 13.66%, 24.12%, 30.43% and 13.23%, 32.62%, 40.48%; after 5 days, 10 days and 15 days successive treatment, respectively (Fig. 5c and d). The generation of superoxide anion and activation of NADPH oxidase was observed to increase significantly ($P<0.05$) in lymphocytes due to *P. berghei* infection. The activated NADPH oxidase transports electrons from NADPH on the cytoplasmic side of the membrane to oxygen in the extracellular fluid to form $\text{O}_2^{\bullet-}$. This $\text{O}_2^{\bullet-}$ leads to oxidative damage of macromolecules including lipid, protein, DNA and antioxidant enzymes (Babior et al., 2002). But our study support that nano conjugated chloroquine protect the immune cell through reducing the NADPH oxidase activity and excess $\text{O}_2^{\bullet-}$ generation.

Lipid peroxidation is important determinant to assess the cellular damage. Lipid peroxidation in lymphocytes was measured in terms of malondialdehyde (MDA). MDA level decreased significantly ($P<0.05$) by 25.14%, 28.28%, 21.35% respectively as compared to infected control after 100 mg/kg bw, 250 mg/kg bw

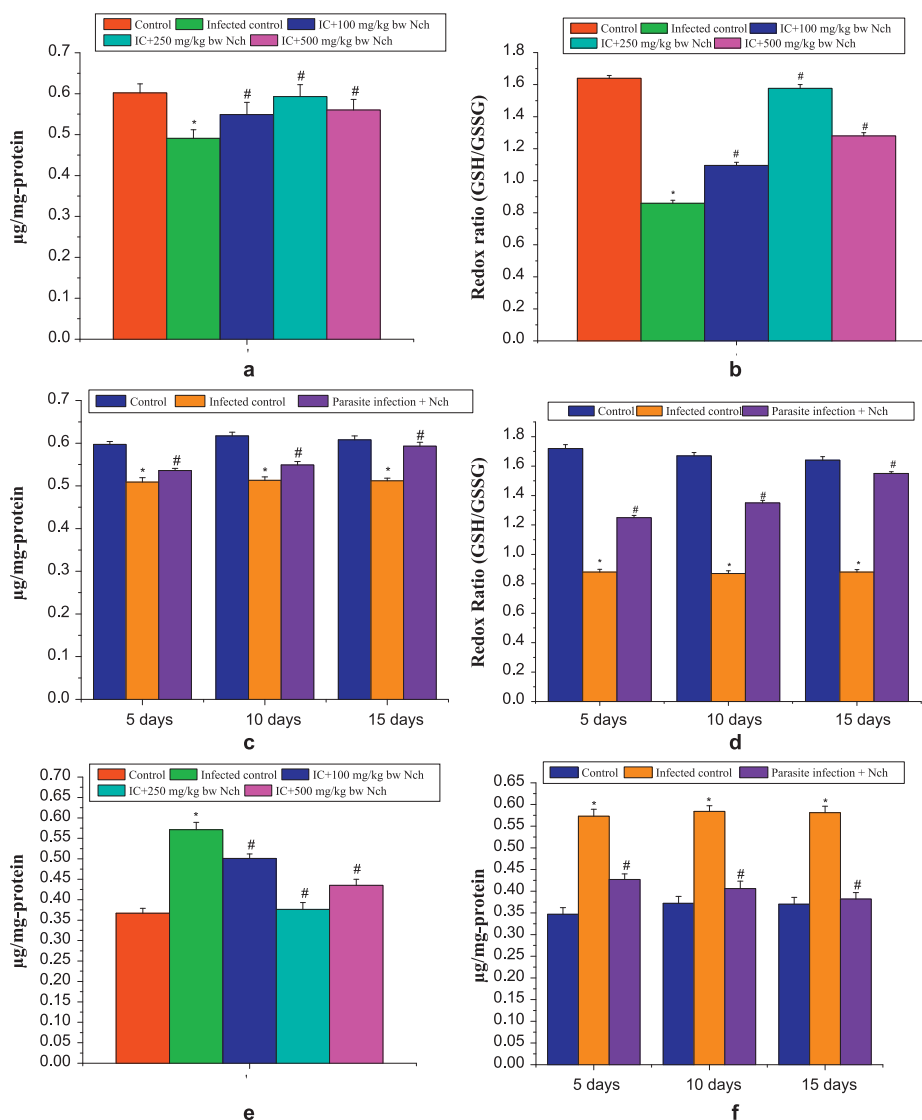


Fig. 7. Graphical presentation of reduced glutathione (GSH) level and redox ratio (a–d); oxidized glutathione (GSSG) activity (e and f) of lymphocytes during effective dose and effective duration study respectively. Values are expressed as mean \pm SEM, $n = 6$. *Significant difference ($P < 0.05$) compared to control group. #Significant difference ($P < 0.05$) compared to infected control group.

and 500 mg/kg bw Nch treatment per day for 10 days successive treatment (Fig. 5e). MDA level were increased significantly ($P < 0.05$) by 53.94%, 59.98%, 55.34% in infected group, respectively, after 5 days, 10 days and 15 days of infection. Treatment of 250 mg/kg bw/day nanoconjugated chloroquine in infected group decreased MDA level significantly ($P < 0.05$) by 19.64%, 26.84%, 32.89% after 5 days, 10 days and 15 days successive treatment, respectively (Fig. 5f).

ROS arise from the production of nitric oxide and oxygen radicals produced by the host's immune system in response to iRBC bursting and merozoite release (Becker et al., 2004). *P. berghei* infected mice blood lymphocyte showed the significantly ($P < 0.05$) increasing of NO generation from infected group as compared to control group but Nch supplementation in different concentration decreased the NO generation (Fig. 6a). NO release in serum was found to be increase significantly ($P < 0.05$) in infected group, but it also decreased after Nch supplementation (Fig. 6b). NO generation and release were increased significantly ($P < 0.05$) by 108.34%, 108.58%, 110.45% and 54.83%, 55.5%, 52.75% in *P. berghei* infected group, respectively, after 5 days, 10 days and 15 days of

infection. Treatment of 250 mg/kg bw/day Nch in *P. berghei* infected group decreased NO generation and release significantly ($P < 0.05$) by 10.26%, 22.4%, 39.32% and 13.37%, 19.19%, 28.33%; respectively (Fig. 6c and d).

Glutathione is an important antioxidant in cellular system. The plasmodium GSH pathway, in conjunction with the thioredoxin redox system, could indeed act as a primary line of defense against oxidative damage (Salinas et al., 2004). So, to understand glutathione level, we have measured both reduced glutathione and redox ratio. Treatment with nano conjugated chloroquine increased the reduced glutathione (GSH) level in Group III, Group IV, Group V by 11.81%, 20.77%, 14.05% and 27.47%, 83.58%, 49.01% respectively when compared with infected group (Fig. 7a and b). Treatment of 250 mg/kg bw/day nanoconjugated chloroquine for 5, 10, 15 days in *P. berghei* infected group, GSH level and also redox ratio increased by 5.3%, 7.01%, 15.82% and 42.04%, 55.17%, 76.13% respectively (Fig. 7c and d). The GSSG level was also decreased in treated group then infected group. In Fig. 7e, the dose of 250 mg/kg bw showed the effect 34.15%, 100 mg/kg bw showed 13.97% and 500 mg/kg bw showed 15.06%. During 5, 10 and 15 days treatment

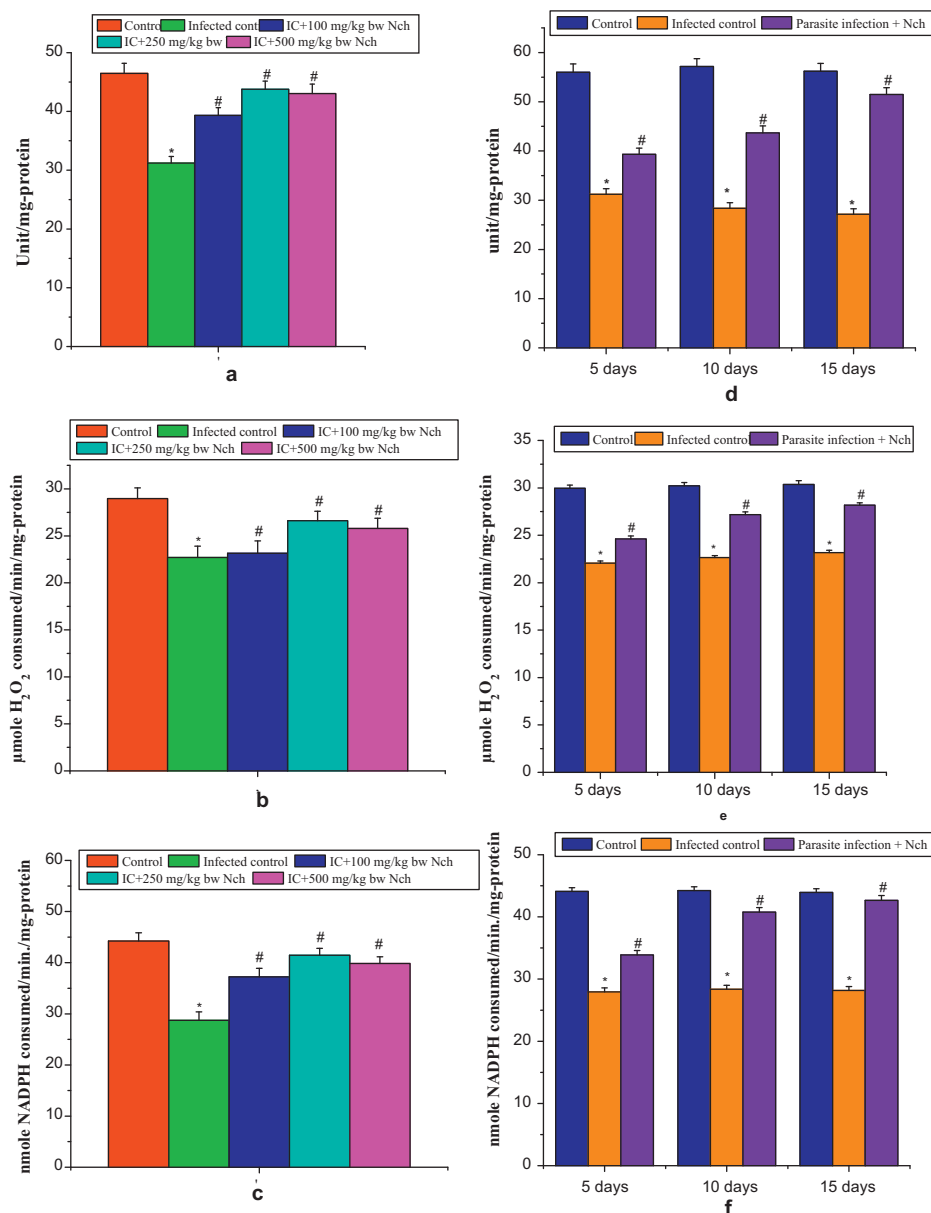


Fig. 8. Graphical presentation of superoxide dismutase (SOD) activity (a and d); catalase activity (b and e); glutathione reductase (GR) activity (c and f); of lymphocytes during effective dose and effective duration study respectively. Values are expressed as mean \pm SEM, $n = 6$. *Significant difference ($P < 0.05$) compared to control group. #Significant difference ($P < 0.05$) compared to infected control group.

schedule the GSSG level significantly decreased ($P < 0.05$) by 25.47%, 30.47%, 34.25% respectively (Fig. 7f).

The superoxide dismutase (SOD), catalase (CAT), glutathione reductase (GR) activity were measured to understand the antioxidant status of different group of lymphocytes. The activity of antioxidant (SOD, CAT and GR) enzymes were decreased (32.85%, 21.58%, 35.02% respectively) significantly ($P < 0.05$) when compared to their control. These antioxidant activities were significantly ($P < 0.05$) rose in Nch supplemented group as compared to their infected group. Among the different concentrations of Nch, 250 mg/kg bw is the most effective dose (SOD: 56.27%, CAT: 17.16%, GR: 44.18%) to play a protective role against the *P. berghei* infection (Fig. 8a–c). SOD, CAT, and GR activity were decreased significantly ($P < 0.05$) by 26.05%, 35.01%, 89.58%; 11.65%, 20.00%, 21.57%; and 21.26%, 43.67%, 51.29% in *P. berghei* infected group, respectively, after 5 days, 10 days and 15 days of nanoconjugated

chloroquine treatment (Fig. 8d–f) and for 15 days treatment is more effective.

Imbalance between the generation of reactive oxygen species (ROS) and the antioxidant system causes oxidative stress. Immune cell uses ROS to carry out many of its functions. It needs appropriate levels of intracellular antioxidants to eliminate the harmful effect of ROS. Glutathione is a crucial component of the antioxidant defense mechanism, and it functions as a direct reactive free radical scavenger (Sarkar et al., 1995). In the study decreased GSH level may be due to increasing level of lipid oxidation products which may be associated with less availability of NADPH required for activity of GR to transform GSSG to GSH due to increase production of ROS at a rate that exceeds ability to regenerate GSH in lymphocytes with infection (Ray and Hussain, 2002). SOD, a chain breaking antioxidant, plays an important role in protection against deleterious effects of lipid peroxidation (Sullivan et al., 2000).

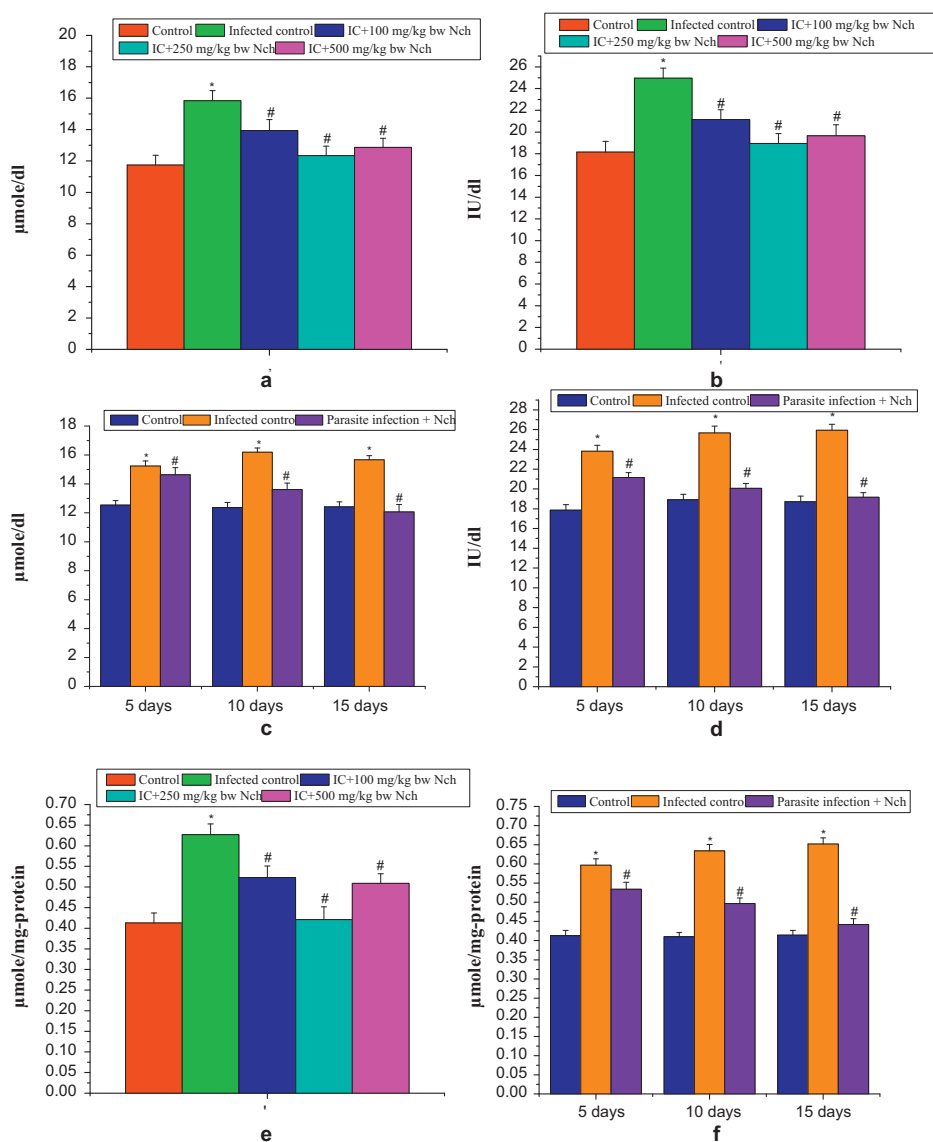


Fig. 9. Graphical presentation of C-reactive protein level (a and c); lactate dehydrogenase (LDH) level (b and d); and myeloperoxidase activity (e and f) of serum during effective dose and effective duration study respectively. Values are expressed as mean \pm SEM, $n=6$. *Significant difference ($P<0.05$) compared to control group. #Significant difference ($P<0.05$) compared to infected control group.

CRP and LDH level were significantly ($P<0.05$) increased in serum of *P. berghei* infected mice blood as compared to respective control groups and after Nch treatment the LDH level and CRP activity significantly ($P<0.05$) decreased by 11.94%, 22.04%, 18.71% and 15.22%, 24.07%, 21.23% in treated groups during effective dose study (Fig. 9a and b). During effective duration study CRP and LDH level significantly ($P<0.05$) decreased by 3.93%, 15.87%, 23.03% and 10.55%, 21.60%, 32.2% respectively (Fig. 9c and d). MPO is an important enzyme to produce hypochlorous acid in cellular system that leads to oxidative damage. So, it is an important determinant to establish the free radical generation in *P. berghei* infection. MPO activity is significantly ($P<0.05$) increased in infected group. Nch, 100 mg/kg bw, 250 mg/kg bw, 500 mg/kg bw decreased the MPO activity significantly ($P<0.05$) by 16.58%, 32.85%, 18.82% compared to their infected group (Fig. 9e). Serum MPO activity were increased significantly ($P<0.05$) by 44.55%, 54.63%, 57.48% in *P. berghei* infected group, respectively, after 5 days, 10 days and 15 days of infection. Treatment of 250 mg/kg bw/day nanoconjugated chloroquine in infected group decreased MPO activity significantly ($P<0.05$) by 10.55%, 21.60%, 32.2%; after 5 days, 10 days and 15 days

successive treatment, respectively (Fig. 9f). In the presence of serum derived MPO, ROS generates hypochlorous acid (HOCl) and initiate the deactivation of antiproteases and the activation of latent proteases, that leads to the tissue damage (Kapoor and Banyal, 2011). In our study, Nch supplementation also inhibits the MPO activity which was increased due to malaria parasite infection; suggest that protective role of Nch.

SGOT and SGPT activity were significantly ($P<0.05$) increased in serum of *P. berghei* infected mice blood, as compared to its control. 100, 250, 500 mg/kg bw/day Nch supplementation among three concentration drugs showed the effect of decreasing the SGOT and SGPT level in treated groups by 10.09%, 24.07%, 20.76% and 6.72%, 29.81%, 22.99% respectively, as compared to its infected groups (Fig. 10a and b). SGOT, and SGPT level were increased significantly ($P<0.05$) by 52.45%, 55.13%, 53.49%; and 53.82%, 57.31%, 55.59% in *P. berghei* infected group, respectively. After 5 days, 10 days and 15 days of nanoconjugated chloroquine treatment, SGOT and SGPT level were decreased significantly ($P<0.05$) by 16.17%, 26.82%, 31.28%; and 22.62%, 27.92%, 31.92% respectively (Fig. 10c and d).

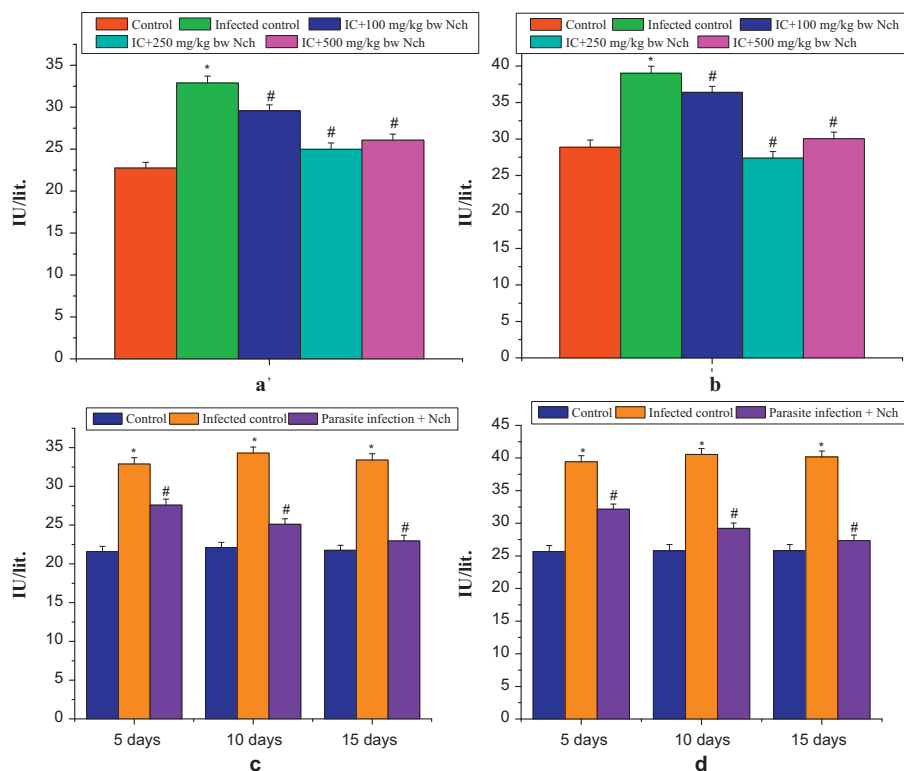


Fig. 10. Serum glutamate oxalate transaminase (SGOT) level (a and c); serum glutamate pyruvate transaminase (SGPT) level (b and d); during effective dose and effective duration study respectively. Values are expressed as mean \pm SEM, $n = 6$. *Significant difference ($P < 0.05$) compared to control group. #Significant difference ($P < 0.05$) compared to infected control group.

4. Conclusion

The study demonstrate that, ionically cross-linked CS–TPP nanoparticles act as drug delivery vehicles against rodent parasite and CS–TPP NP containing chloroquine, potentially eliminate parasite and protects the lymphocytes, serum and RBC against *P. berghei* infection at the dose of 250 mg/kg bw/day for 15 days maximally by decreasing free radical generation, lipid and protein damage, and also by increasing the antioxidant status. Hence, the nanoconjugated chloroquine may be used as a potential therapeutic antimalarial agent, a free radical scavenger and antioxidative product against malaria infection. However, further studies are necessary to clarify the relationship between the parasite load in the host, and also Nch bioavailability and/or its effectiveness against chloroquine resistant parasite (this research will be reported in our next-coming publication), and the host responses, including immune mechanisms in the course of medication.

Conflicts of interest

The authors declare that there are no conflicts of interest.

Acknowledgements

The authors express gratitude to the Indian Institute of Technology, Kharagpur and Vidyasagar University, Midnapore for providing the facilities to execute these studies.

References

Babior, B.M., Lambeth, J.D., Nauseef, W., 2002. The neutrophil NADPH oxidase. Arch. Biochem. Biophys. 397, 342–344.

- Bawa, R., Bawa, S.R., Maebius, S.B., Flynn, T., Wei, C., 2005. Protecting new ideas and inventions in nanomedicine with patents. Nanomed. Nanotechnol. Biol. Med. 1, 150–158.
- Becker, K., Tilley, L., Vennerstrom, J.L., Roberts, D., Rogerson, S., Ginsburg, H., 2004. Oxidative stress in malaria parasite-infected erythrocytes: host–parasite interactions. Int. J. Parasitol. 34, 163–189.
- Cevher, E., Orhan, Z., Mulazimoglu, L., Sensoy, D., Alper, M., Yildiz, A., Ozsoy, Y., 2006. Characterization of biodegradable chitosan microspheres containing vancomycin and treatment of experimental osteomyelitis caused by methicillin-resistant *Staphylococcus aureus* with prepared microspheres. Int. J. Pharm. 317, 127–135.
- Chakraborty, S.P., Sahu, S.K., KarMahapatra, S., Santra, S., Bal, M., Roy, S., Pramanik, P., 2010. Nanoconjugated vancomycin: new opportunities for the development of anti-VRSA agents. Nanotechnology 21 (ID 105103).
- Chakraborty, S.P., KarMahapatra, S., Sahu, S., Das, S., Tripathy, S., Dash, S., Pramanik, P., Roy, S., 2011a. Internalization of *Staphylococcus aureus* in lymphocytes induces oxidative stress and DNA fragmentation: possible ameliorative role of nanoconjugated vancomycin. Oxid. Med. Cell. Long., 15, <http://dx.doi.org/10.1155/2011/942123>.
- Chakraborty, S.P., Sahu, S.K., Pramanik, P., Roy, S., 2011b. Biocompatibility of folate-modified chitosan nanoparticles. Asian Pac. J. Trop. Biomed. 2, 215–219.
- Francis, S.E., Sullivan, D.J., Goldberg, D.E., 1997. Hemoglobin metabolism in the malaria parasite *Plasmodium falciparum*. Annu. Rev. Microbiol. 51, 97–123.
- Goldstein, I.M., Cerqueira, M., Lond, S., Kaplan, H.B., 1977. Evidence that the superoxide generating system of human leukocytes is associated with the cell surface. J. Clin. Invest. 59, 249–254.
- Guinovart, C., Navia, M.M., Tanner, M., Alonso, P.L., 2006. Malaria: burden of disease. Curr. Mol. Med. 6, 137–140.
- Gupta, S., Saxena, K.C., 1980. In vitro hemolytic activity of *Plasmodium berghei* on red blood cells. J. Biosci. 2, 129–134.
- Heyneman, R.A., Vercauteren, R.E., 1984. Activation of a NADPH oxidase from horse polymorphonuclear leukocytes in a cell-free system. J. Leukoc. Biol. 36, 751–759.
- Holmgren, A., Bjornstedt, T.M., 1995. Thioredoxin and thioredoxin reductase. Methods Enzymol. 252, 199–208.
- Joshi, M., Pathak, S., Sharma, S., Patravale, V., 2008. Design and *in vivo* pharmacodynamic evaluation of nanostructured lipid carriers for parenteral delivery of artemether. Nanoject. Int. J. Pharm. 364, 119–126.
- Kapoor, G., Banyal, H.S., 2011. Purification and characterization of *Plasmodium berghei* thioredoxin reductase. Asian J. Anim. Sci. 5, 145–152.
- Kato, Y., Onishi, H., Machida, Y., 2003. Application of chitin and chitosan derivatives in the pharmaceutical field. Curr. Pharm. Biotechnol. 4, 303–309.
- Lam, T.D., Hoang, V.D., Lien, L.N., Thinh, N.N., Dien, P.G., 2006. Synthesis and characterization of chitosan nanoparticles used as a drug carrier. J. Chem. 44, 105–109.

- Lehane, A.M., Kirk, K., 2010. Efflux of a range of antimalarial drugs and chloroquine resistance reversers' from the digestive vacuole in malaria parasites with mutant PfCRT. *Mol. Microbiol.* 77, 1039–1051.
- Lowry, O.H., Rosenbrough, N.J., Farr, A.L., Randall, R.J., 1951. Protein measurement with the Folin phenol reagent. *J. Biol. Chem.* 193, 255–275.
- Mohan, K., Ganguly, N.K., Dubey, M.L., Mahajan, R.C., 1992. Oxidative damage of erythrocyte infected with *Plasmodium falciparum*. An in vitro study. *Ann. Hematol.* 65, 131–134.
- Paliwal, R., Paliwal, S.R., Agrawal, G.P., Vyas, S.P., 2012. Chitosan nanoconstructs for improved oral delivery of low molecular weight heparin: in vitro and in vivo evaluation. *Int. J. Pharm.* 422, 179–184.
- Peters, W., Portus, J.H., Robinson, B.L., 1975. The chemotherapy of rodent malaria. XXII. The value of drug-resistant strains of *P. berghei* in screening for blood schizontocidal activity. *Ann. Trop. Med. Parasitol.* 69, 155–171.
- Ray, G., Hussain, S.A., 2002. Oxidants, antioxidants and carcinogenesis. *Indian J. Exptl. Biol.* 40, 1213–1235.
- Reitman, S., Frankel, S.A., 1957. Colorimetric method for the determination of serum glutamic oxalacetic and glutamic pyruvic transaminases. *Am. J. Clin. Pathol.* 28, 56–63.
- Romao, P.R., Tovar, J., Fonseca, S.G., Moraes, R.H., Cruz, A.K., Hothersall, J.S., 2006. Glutathione and the redox control system trypanothione/trypanothione reductase are involved in the protection of *Leishmania* sp. against nitrosothiol-induced cytotoxicity. *Braz. J. Med. Biol. Res.* 39, 355–363.
- Salinas, G., Selkirk, M.E., Chalar, C., Maizels, R.M., Fernandez, C., 2004. Linked thioredoxin–glutathione systems in platyhelminths. *Trends Parasitol.* 20, 340–346.
- Sandhu, S.K., Kaur, G., 2002. Alterations in oxidative stress scavenger system in aging rat brain and lymphocytes. *Biogerontology* 3, 161–173.
- Sarkar, S., Yadav, P., Trivedi, R., Bansal, A.K., Bhatnagar, D., 1995. Cadmium-induced lipid peroxidation and the status of the antioxidant system in rat tissues. *J. Elem. Med.* 9, 144–147.
- Sharma, V.P., 2007. Battling the malaria iceberg with chloroquine in India. Battling the malaria iceberg with chloroquine in India. *Malaria J.* 6, <http://dx.doi.org/10.1186/1475-2875-6-105>.
- Shu, X., Zhu, K., 2002. The influence of multivalent phosphate structure on the properties of ionically cross-linked chitosan films for controlled drug release. *Eur. J. Pharm. Biopharm.* 54, 235–243.
- Soma, C.E., Dubernet, C., Barratt, G., Benita, S., Couvreur, P., 2000. Investigation of the role of macrophages on the cytotoxicity of doxorubicin and doxorubicin-loaded nanoparticles on M5076 cells in vitro. *J. Control. Release* 68, 283–289.
- Sullivan, G.W., Sarembock, I.J., Linden, J., 2000. The role of inflammation in vascular diseases. *J. Leukoc. Biol.* 67, 591–602.
- Swai, H., Semete, B., Kalombo, L., Chelule, P., 2008. Potential of treating tuberculosis with a polymeric nano-drug delivery system. *J. Control. Release* 132, e48.
- Takla, P.G., Dakas, C.J., 2002. A study of interactions of chloroquine with ethanol, sugars and glycerol using ultraviolet spectrophotometry. *Int. J. Pharm.* 43, 225–232, [http://dx.doi.org/10.1016/0378-5173\(88\)90278-5](http://dx.doi.org/10.1016/0378-5173(88)90278-5).
- Tripathy, S., Chakraborty, S.P., Roy, S., 2012. Superoxide radical generation mediated *Plasmodium berghei* infection in Swiss mice. *Al Ameen J. Med. Sci.* 5, 69–81.
- Wang, T., Hu, Y., Leach, K.M., Zhang, L., Yang, W., Jiang, L., Feng, Z.Q., He, N., 2012. Erythropoietin-loaded oligochitosan nanoparticles for treatment of periventricular leukomalacia. *Int. J. Pharm.* 422, 462–471.